SRG evolution of transition operators and currents (and connections to factorization)

Sushant N. More

National Superconducting Cyclotron Laboratory
Michigan State University

INT, June 2017

Collaborators: Dick Furnstahl, Scott Bogner, Sebastian König, Kai Hebeler

Outline

1. Nuclear structure vs. reaction
2. Test Case: Deuteron electrodisintegration
   - Scale dependence and kinematics
   - Final state evolution
   - Operator evolution
   - D-state scale dependence
3. Summary and Takeaways
4. Relation to $0\nu\beta\beta$

Nuclear structure vs. reaction

- Traditionally, nuclear structure treated separately from nuclear reactions. Assumes unique factorization of structure and reaction components.
- Extract nuclear properties from experiments and predict them with theory.
- $\frac{d\sigma}{d\Omega} \propto \left| \langle \psi_{\rm final} \,|\, \hat{O}(q) \,|\, \psi_{\rm initial} \rangle \right|^2$
- $\langle \underbrace{\psi_{\rm final}}_{\rm structure} \,|\, \overbrace{\hat{O}(q)}^{\rm reaction} \,|\, \underbrace{\psi_{\rm initial}}_{\rm structure} \rangle$

Nucleon knockout reaction

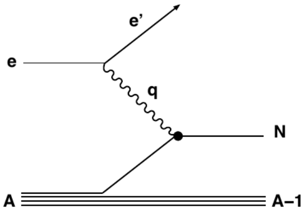

Nuclear structure vs. reaction

- Traditionally, nuclear structure treated separately from nuclear reactions. Assumes unique factorization of structure and reaction components.
- Extract nuclear properties from experiments and predict them with theory.
- $\frac{d\sigma}{d\Omega} \propto \left| \langle \psi_{\text{final}} \,|\, \hat{O}(q) \,|\, \psi_{\text{initial}} \rangle \right|^2$
- $\langle \underbrace{\psi_{\text{final}}}_{\text{structure}} \,|\, \overbrace{\hat{O}(q)}^{\text{reaction}} \,|\, \underbrace{\psi_{\text{initial}}}_{\text{structure}} \rangle$
- Use factorization to isolate individual components and extract process-independent nuclear properties.

Nucleon knockout reaction

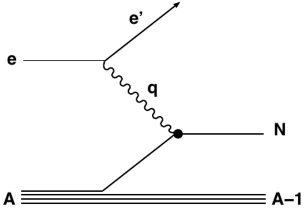

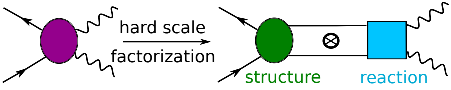

Factorization: Examples

High-E QCD

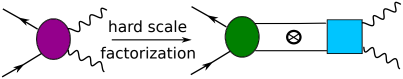

$$F_2(x, Q^2) \sim \sum_a f_a(x, \mu_f) \otimes \widehat{F}_2^a(x, Q/\mu_f)$$

long-distance parton density

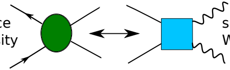

short-distance Wilson coefficient

- Separation between long- and short-distance physics is not unique, but defined by the scale μ_f
- Form factor F_2 is independent of μ_f, but pieces are not
- $f_a(x, \mu_f = Q^2)$ runs with Q^2, but is process independent

Low-E Nuclear

Observable: cross section

Structure model: spectroscopic factor

Reaction model: single-particle cross section

$$\sigma^{if} = \sum_{|J_i - J_f| \leq j \leq J_i + J_f} S_j^{if} \sigma_{sp}$$

Factorization: Examples

High-E QCD

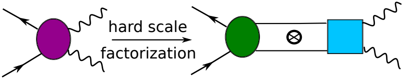

$$F_2(x, Q^2) \sim \sum_a f_a(x, \mu_f) \otimes \widehat{F}_2^a(x, Q/\mu_f)$$

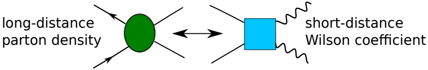

- Separation between long- and short-distance physics is not unique, but defined by the scale μ_f
- Form factor F_2 is independent of μ_f, but pieces are not
- $f_a(x, \mu_f = Q^2)$ runs with Q^2, but is process independent

Low-E Nuclear

Observable: cross section

Structure model: spectroscopic factor

Reaction model: single-particle cross section

$$\sigma^{if} = \sum_{|J_i - J_f| \leq j \leq J_i + J_f} S_j^{if} \sigma_{sp}$$

Open questions

- When does factorization hold?
- Which process-independent nuclear properties can we extract?
- What is the scale/scheme dependence of the extracted properties?

Scale-scheme dependence: QCD vs. low-E nuclear

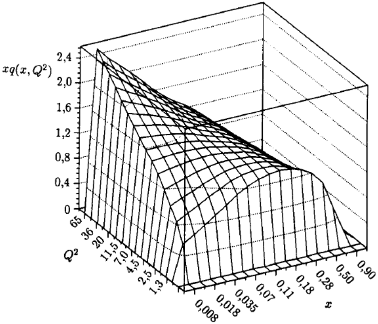

- $x\,q(x,\, Q^2)$: share of momentum carried by quarks in particular x-interval
- The quark distribution $q(x,\, Q^2)$ is scale and scheme dependent
- $q(x,\, Q^2)$ and $q(x,\, Q_0^2)$ are related by RG evolution equations

Scale-scheme dependence: QCD vs. low-E nuclear

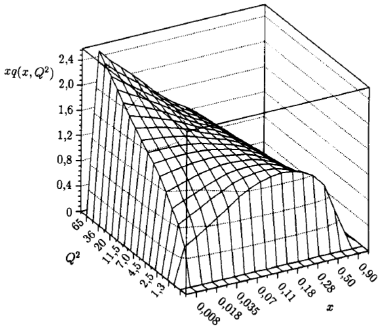

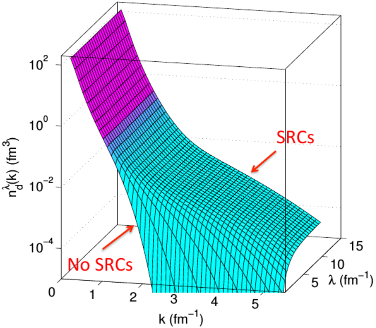

- $x\,q(x,\,Q^2)$: share of momentum carried by quarks in particular x-interval
- The quark distribution $q(x,\,Q^2)$ is scale and scheme dependent
- $q(x,\,Q^2)$ and $q(x,\,Q_0^2)$ are related by RG evolution equations

- AV18 potential evolved from $\lambda = \infty$ to $\lambda = 1.5\,\mathrm{fm}^{-1}$
- Deuteron momentum distribution is scale and scheme dependent
- High momentum tail shrinks as λ decreased (lower resolution)

Scale and scheme choice

- Scheme in low-E nuclear physics: choice of potential, regulators, RG evolution . . .

How do we choose a scale/ scheme?

- Make calculations easier/ more convergent
- Does simple structure always imply a complicated reaction calculation?
- Clean extraction from experiments; increased validity of impulse approximation
- Correctly use the structure information in other processes
- Better interpretation/ intuition
  $\rightarrow$ Surrey group: sensitivity to high-*np* momenta and D-state component in (d,p) reactions [e.g., PRL **117** (2016)]
  $\rightarrow$ JLab SRC/EMC correlation experiments [e.g., Hen et al., RMP]

Scale and scheme choice

- Scheme in low-E nuclear physics: choice of potential, regulators, RG evolution . . .

How do we choose a scale/ scheme?

- Make calculations easier/ more convergent
- Does simple structure always imply a complicated reaction calculation?
- Clean extraction from experiments; increased validity of impulse approximation
- Correctly use the structure information in other processes
- Better interpretation/ intuition
  $\rightarrow$ Surrey group: sensitivity to high-*np* momenta and D-state component in (d, p) reactions [e.g., PRL **117** (2016)]
  $\rightarrow$ JLab SRC/EMC correlation experiments [e.g., Hen et al., RMP]

Use renormalization group (RG) as a tool to consistently relate scales and quantitatively probe ambiguities

SRG makes scale dependence obvious

- SRG scale λ sets the scale for decoupling high- and low-momentum *and* separating structure and reaction

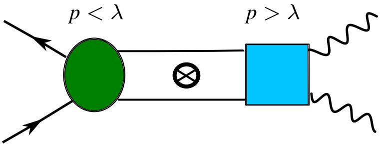

SRG makes scale dependence obvious

- SRG scale λ sets the scale for decoupling high- and low-momentum *and* separating structure and reaction
- Transformed wave function $\rightarrow$ no high momentum components (no SRC)
- $\sigma \sim \left|\langle\psi_f|\hat{O}_q|\psi_i\rangle\right|^2 \Rightarrow \hat{O}_q$ must change to keep observables invariant
- UV physics absorbed in operator (cf. Chiral EFTs)

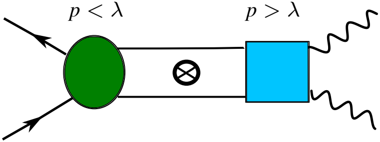

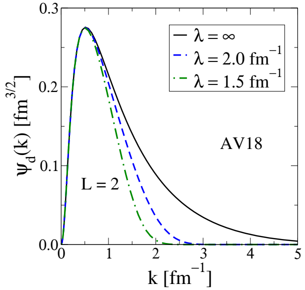

SRG makes scale dependence obvious

- SRG scale λ sets the scale for decoupling high- and low-momentum *and* separating structure and reaction
- Transformed wave function $\rightarrow$ no high momentum components (no SRC)
- $\sigma \sim \left|\langle\psi_f|\hat{O}_q|\psi_i\rangle\right|^2 \Rightarrow \hat{O}_q$ must change to keep observables invariant
- UV physics absorbed in operator (cf. Chiral EFTs)
- $\langle\psi_f|\hat{O}_q|\psi_i\rangle = \langle\psi_f^\lambda|\hat{O}_q^\lambda|\psi_i^\lambda\rangle$
  Naive expectation: RG changes to $\hat{O}_q$ complicates reaction calculations

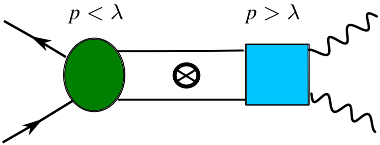

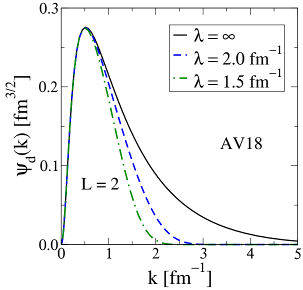

1. Nuclear structure vs. reaction

2. Test Case: Deuteron electrodisintegration
   - Scale dependence and kinematics
   - Final state evolution
   - Operator evolution
   - D-state scale dependence

3. Summary and Takeaways

4. Relation to $0\nu\beta\beta$

Test ground: $^2\mathrm{H}\,(e, e'\ \mathrm{p})\,\mathrm{n}$

- Use deuteron disintegration to investigate scale/ scheme dependence of factorization
- $^2\mathrm{H}\,(e, e'\ \mathrm{p})\,\mathrm{n}$: simplest knockout process. Has many of the essential ingredients and no complications
- No induced 3N forces or currents
- Well-studied experimentally

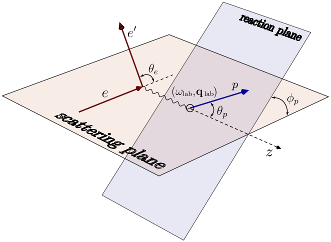

Test ground: ^{2}H $(e, e'$ p) n

- Use deuteron disintegration to investigate scale/ scheme dependence of factorization
- ^{2}H $(e, e'$ p) n: simplest knockout process. Has many of the essential ingredients and no complications
- No induced 3N forces or currents
- Well-studied experimentally

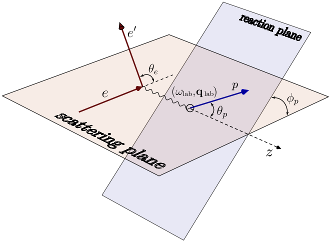

- $\frac{d\sigma}{d\Omega} \propto (v_L f_L + v_T f_T + v_{TT} f_{TT} \cos 2\phi_p + v_{LT} f_{LT} \cos \phi_p)$
- $v_L,\ v_T, \ldots$- electron kinematic factors. $f_L,\ f_T, \ldots$- deuteron structure functions

Test ground: ^{2}H $(e, e'$ p) n

- Use deuteron disintegration to investigate scale/ scheme dependence of factorization
- ^{2}H $(e, e'$ p) n: simplest knockout process. Has many of the essential ingredients and no complications
- No induced 3N forces or currents
- Well-studied experimentally

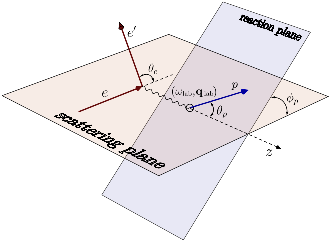

- $$\frac{d\sigma}{d\Omega} \propto (v_L f_L + v_T f_T + v_{TT} f_{TT} \cos 2\phi_p + v_{LT} f_{LT} \cos \phi_p)$$
- $v_L,\ v_T, \ldots$- electron kinematic factors. $f_L,\ f_T, \ldots$- deuteron structure functions

Deuteron disintegration calculations

following Yang, Phillips (2013)

[H. Ibrahim]

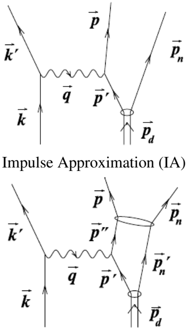

Impulse Approximation (IA)

Final State Interactions (FSI)

- Calculate longitudinal structure function
  $f_L \sim \sum_{m_s, m_J} \left| \langle \psi_f | J_0 | \psi_i \rangle \right|^2$
- $|\psi_f\rangle = \underbrace{|\phi\rangle}_{\text{IA}} + \underbrace{G_0\, t\, |\phi\rangle}_{\text{FSI}}$
  G_0 : Green's function. t : t-matrix

Deuteron disintegration calculations

following Yang, Phillips (2013)

[H. Ibrahim]

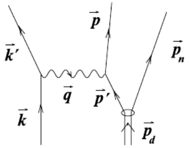

Impulse Approximation (IA)

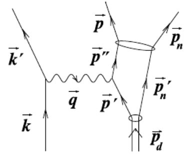

Final State Interactions (FSI)

- Calculate longitudinal structure function
  $f_L \sim \sum_{m_s, m_J} \left| \langle \psi_f | J_0 | \psi_i \rangle \right|^2$
- $|\psi_f\rangle = \underbrace{|\phi\rangle}_{\text{IA}} + \underbrace{G_0\, t\, |\phi\rangle}_{\text{FSI}}$
  G_0 : Green's function. t : t-matrix

- $f_L^\lambda \sim \left| \underbrace{\langle \psi_f | U_\lambda^\dagger}_{\psi_f^\lambda} \underbrace{U_\lambda\, J_0\, U_\lambda^\dagger}_{J_0^\lambda} \underbrace{U_\lambda\, |\psi_i\rangle}_{\psi_i^\lambda} \right|^2; \quad U_\lambda^\dagger U_\lambda = I; \quad f_L^\lambda = f_L$
- Components depend on the scale λ. Cross section does not!

Evolutionary effects

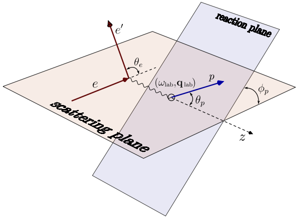

- ^{2}H$(e, e'$ p) n calculations done using AV18 potential with $\lambda = \infty$ and $\lambda = 1.5$ fm^{-1}
- $f_L \sim \sum_{m_s, m_J} \left|\langle \psi_f | J_0 | \psi_i \rangle\right|^2$
- Effects due to evolution of one or more components of $\langle \psi_f | J_0 | \psi_i \rangle$ as a function of kinematics → scale dependence of factorization
- Proof of principle calculations using simplified J_0. Comparison to experiment not warranted

Evolutionary effects

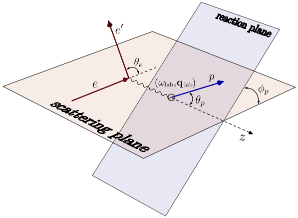

- ^{2}H $(e, e'$ p) n calculations done using AV18 potential with $\lambda = \infty$ and $\lambda = 1.5$ fm^{-1}
- $f_L \sim \sum_{m_s, m_J} \left| \langle \psi_f | J_0 | \psi_i \rangle \right|^2$
- Effects due to evolution of one or more components of $\langle \psi_f | J_0 | \psi_i \rangle$ as a function of kinematics $\rightarrow$ scale dependence of factorization
- Proof of principle calculations using simplified J_0. Comparison to experiment not warranted
- Quasi-free ridge (QFR): $\omega_{\rm photon} = 0$

Evolutionary effects

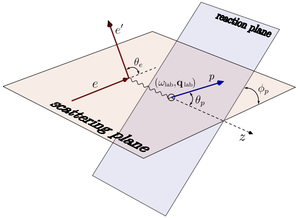

- ^{2}H $(e, e'$ p) n calculations done using AV18 potential with $\lambda = \infty$ and $\lambda = 1.5$ fm^{-1}
- $f_L \sim \sum_{m_s, m_J} \left| \langle \psi_f | J_0 | \psi_i \rangle \right|^2$
- Effects due to evolution of one or more components of $\langle \psi_f | J_0 | \psi_i \rangle$ as a function of kinematics → scale dependence of factorization
- Proof of principle calculations using simplified J_0. Comparison to experiment not warranted
- Quasi-free ridge (QFR): $\omega_{\rm photon} = 0$
- Weak scale dependence at QFR which gets progressively stronger away from it

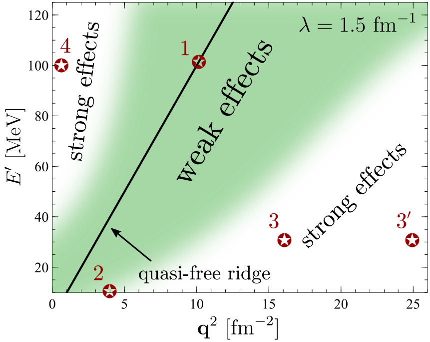

SNM et al., PRC **92**, 064002 (2015)

Evolutionary effects

- Can get away with inconsistent calculations at the quasi-free ridge (QFR)
- Long-range part of the wave function/ on-shell t-matrix probed at QFR
  $\rightarrow$ invariant under SRG evolution
- Scale dependence qualitatively different above and below the QFR
- Can be explained by looking at the effect of evolution on the overlap matrix elements [SNM et al., PRC **92**, 064002 (2015)]

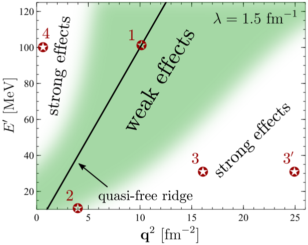

Evolution effects on individual components

- $f_L \propto \sum_{m_s, m_J} \langle \psi_f | J_0 | \psi_i \rangle = \sum_{m_s, m_J} \langle \psi_f^\lambda | J_0^\lambda | \psi_i^\lambda \rangle$
- Looked at effects of evolution on the observable f_L
- Look at changes due to evolution for individual components and their implications
- Evolution of ψ_{deut}: suppression of high-momentum components $\rightarrow$ accelerated convergence of nuclear structure calculations

Evolving the final state

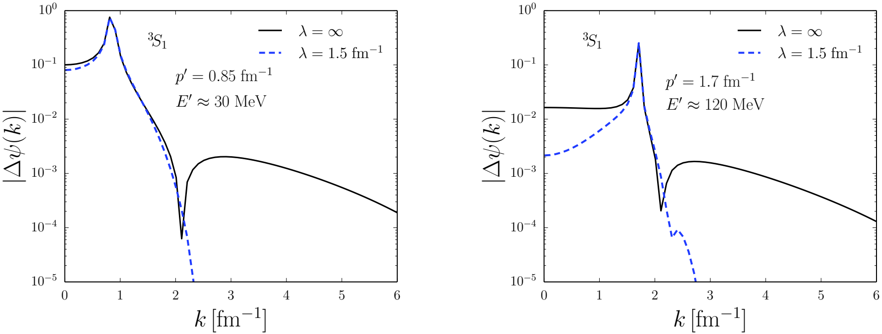

- $\psi_f^{\lambda}(p';k) = \underbrace{\phi_{p'}}_{\text{IA}} + \underbrace{\Delta\psi_{\lambda}(p';k)}_{\text{FSI}}$
- High-k tail suppressed with evolution
- For $p' \gtrsim \lambda$, $\psi_f^{\lambda}(p';k)$ localized around the outgoing momentum p'

r-space ψ_f at different λ

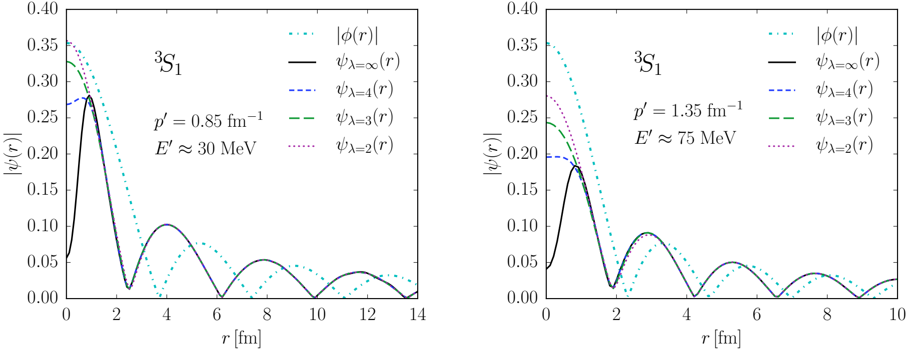

- Small r wound evolved away as λ reduced
- Beyond range of the potential, $\psi(r)$ and $\phi(r)$ differ by phase that is same for all λ

Scale-dependent FSI contribution

- "FSI contribution depends on kinematics"

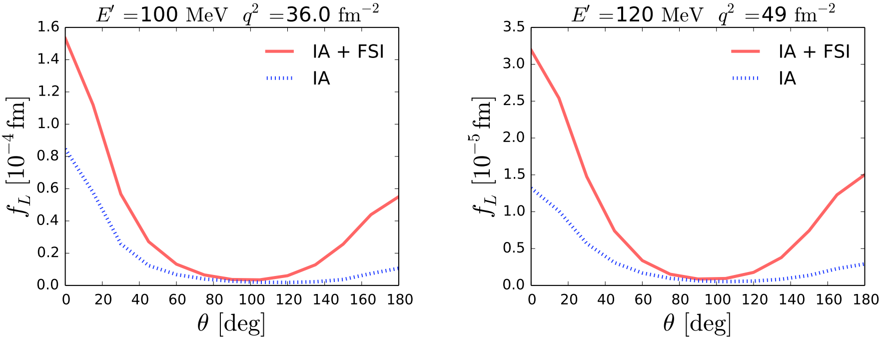

- $\langle \psi_f^\lambda | J_0^\lambda | \psi_i^\lambda \rangle = \langle \phi | J_0^\lambda | \psi_i^\lambda \rangle + \langle \Delta\psi_f^\lambda | J_0^\lambda | \psi_i^\lambda \rangle$
- Local decoupling of $\psi_f^\lambda(k)$ and form of J_0^λ make $\langle \Delta\psi_f^\lambda | J_0^\lambda | \psi_i^\lambda \rangle$ small

Scale-dependent FSI contribution

- "FSI contribution depends on kinematics"

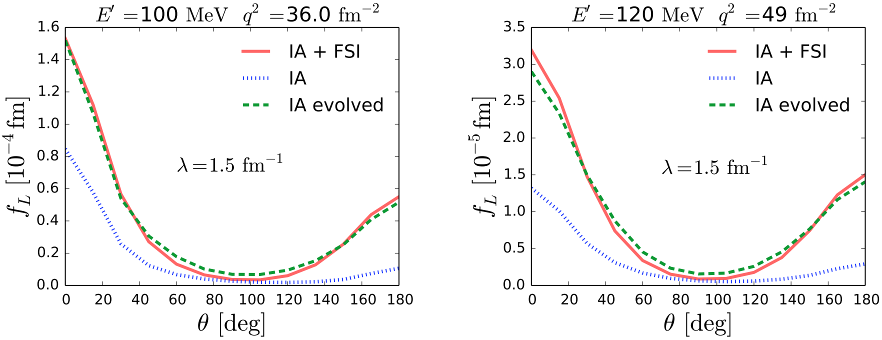

- $\langle \psi_f^\lambda | J_0^\lambda | \psi_i^\lambda \rangle = \langle \phi | J_0^\lambda | \psi_i^\lambda \rangle + \langle \Delta\psi_f^\lambda | J_0^\lambda | \psi_i^\lambda \rangle$
- Local decoupling of $\psi_f^\lambda(k)$ and form of J_0^λ make $\langle \Delta\psi_f^\lambda | J_0^\lambda | \psi_i^\lambda \rangle$ small
- $f_L(\langle \psi_f | J_0 | \psi_i \rangle) \approx f_L(\langle \phi | J_0^\lambda | \psi_i^\lambda \rangle)$

Current evolution story

- $\langle \mathbf{k}_1 T_1 | J_0(\mathbf{q}) | \mathbf{k}_2 T = 0 \rangle =$
$$\frac{1}{2}\left(G_E^p + (-1)_1^T G_E^n\right)\delta(\mathbf{k}_1 - \mathbf{k}_2 - \mathbf{q}/2) + \frac{1}{2}\left((-1)_1^T G_E^p + G_E^n\right)\delta(\mathbf{k}_1 - \mathbf{k}_2 + \mathbf{q}/2)$$

- Varying λ shuffles the physics between short- and long-distance parts
- λ decreases $\rightarrow$ blob size increases. One-body current operator develops two and higher body components

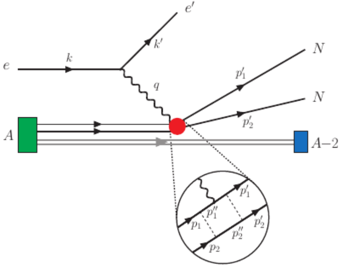

at high resolution

- Naive expectation: RG changes to $J_0(q)$ complicates reaction calculations

EFT for the current

- $\langle \psi_f | J_0(q) | \psi_i \rangle = \langle \psi_f^\lambda | J_0^\lambda(q) | \psi_i^\lambda \rangle$
- Low-momentum component of $J_0^\lambda(q)$ most relevant

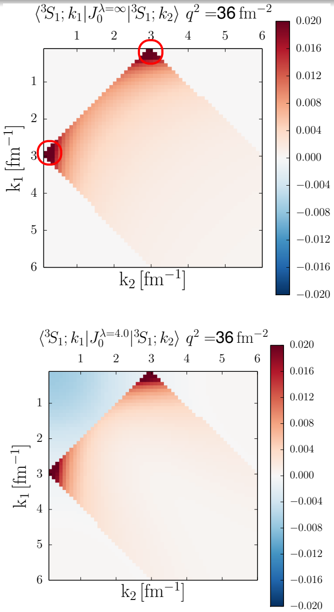

EFT for the current

- $\langle \psi_f | J_0(q) | \psi_i \rangle = \langle \psi_f^\lambda | J_0^\lambda(q) | \psi_i^\lambda \rangle$
- Low-momentum component of $J_0^\lambda(q)$ most relevant

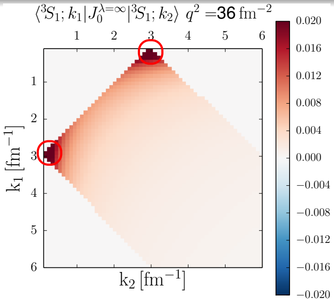

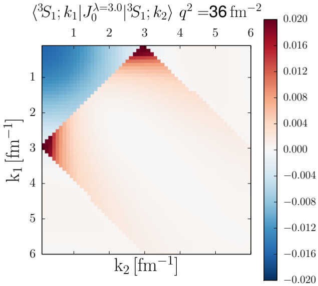

EFT for the current

- $\langle \psi_f | J_0(q) | \psi_i \rangle = \langle \psi_f^\lambda | J_0^\lambda(q) | \psi_i^\lambda \rangle$
- Low-momentum component of $J_0^\lambda(q)$ most relevant

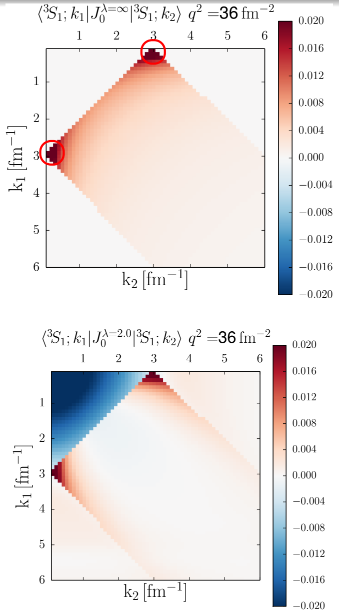

EFT for the current

- $\langle\psi_f|J_0(q)|\psi_i\rangle = \langle\psi_f^\lambda|J_0^\lambda(q)|\psi_i^\lambda\rangle$
- Low-momentum component of $J_0^\lambda(q)$ most relevant

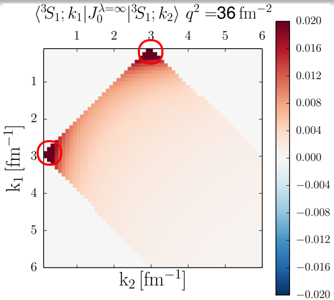

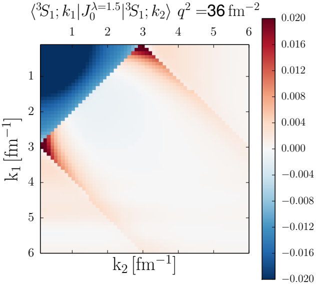

EFT for the current

- $\langle \psi_f | J_0(q) | \psi_i \rangle = \langle \psi_f^\lambda | J_0^\lambda(q) | \psi_i^\lambda \rangle$
- Low-momentum component of $J_0^\lambda(q)$ most relevant
- $\langle {}^3S_1; k_1 | J_0^\lambda(q) | {}^3S_1; k_2 \rangle$ $= g_0^q + g_2^q (k_1^2 + k_2^2) + \cdots$

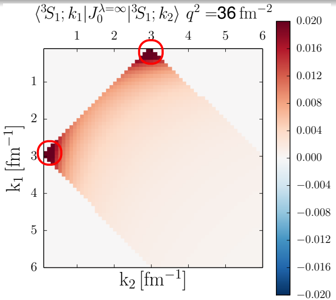

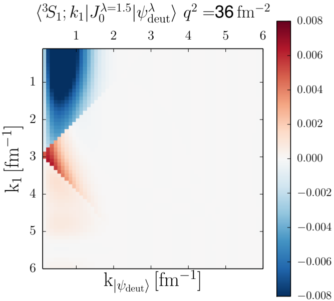

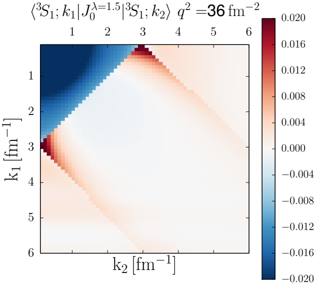

EFT for the current

- $\langle {}^3P_1; k_1 | J_0^\lambda(q) | {}^3S_1; k_2 \rangle = g_1^q\, k_1 + \cdots$
- $\langle {}^3D_2; k_1 | J_0^\lambda(q) | {}^3S_1; k_2 \rangle = g_{2,D}^q\, k_1^2 + \cdots$
- $\langle \psi_f^\lambda | J_0^\lambda(q) | \psi_i^\lambda \rangle \approx \langle \psi_f^\lambda | J_0^\lambda(q) | \psi_{i\,{}^3S_1}^\lambda \rangle$

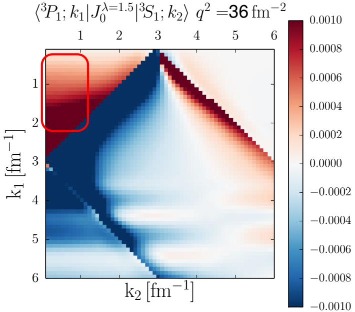

- $\langle \psi_f^\lambda | J_0^\lambda | \psi_{i\,{}^3S_1}^\lambda \rangle =$

$$\langle \psi_f^\lambda | {}^3S_1 \rangle \underbrace{\langle {}^3S_1 | J_0^\lambda | {}^3S_1 \rangle}_{\text{use EFT exp.}} \langle {}^3S_1 | \psi_{i\,{}^3S_1}^\lambda \rangle + \langle \psi_f^\lambda | {}^3P_1 \rangle \underbrace{\langle {}^3P_1 | J_0^\lambda | {}^3S_1 \rangle}_{\text{use EFT exp.}} \langle {}^3S_1 | \psi_{i\,{}^3S_1}^\lambda \rangle + \cdots$$

Results from low-momentum potential

- $\langle \psi_f^\lambda | J_0^\lambda(q) | \psi_{\text{deut}}^\lambda \rangle = g_0^q \; \psi_f^{\lambda\,*}(r)\, \psi_{\text{deut}}^\lambda(r) \Big|_{r=0} + \cdots$

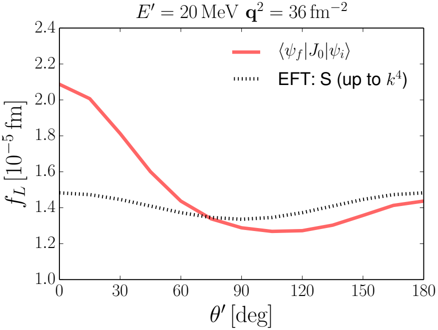

- $\langle \psi_f^\lambda | J_0^\lambda | \psi_{i\,^3S_1}^\lambda \rangle = \langle \psi_f^\lambda | ^3S_1 \rangle \langle ^3S_1 | J_0^\lambda | ^3S_1 \rangle \langle ^3S_1 | \psi_{i\,^3S_1}^\lambda \rangle$

Results from low-momentum potential

- $\langle \psi_f^\lambda | J_0^\lambda(q) | \psi_{\text{deut}}^\lambda \rangle$
  $= g_0^q \; \psi_f^{\lambda *}(r)\, \psi_{\text{deut}}^\lambda(r)\Big|_{r=0} + \cdots$

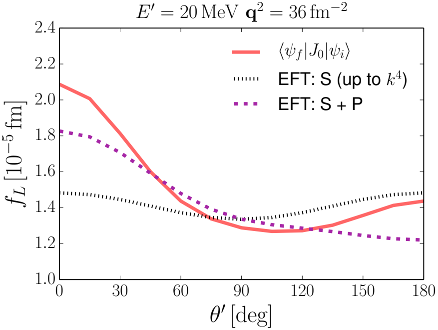

- $\langle \psi_f^\lambda | J_0^\lambda | \psi_{i\,^3S_1}^\lambda \rangle = \langle \psi_f^\lambda | ^3S_1 \rangle \langle ^3S_1 | J_0^\lambda | ^3S_1 \rangle \langle ^3S_1 | \psi_{i\,^3S_1}^\lambda \rangle$
  $+ \sum_{J=0,1,2} \langle \psi_f^\lambda | ^3P_J \rangle \langle ^3P_J | J_0^\lambda | ^3S_1 \rangle \langle ^3S_1 | \psi_{i\,^3S_1}^\lambda \rangle$

Results from low-momentum potential

- $\langle \psi_f^\lambda | J_0^\lambda(q) | \psi_{\text{deut}}^\lambda \rangle = g_0^q \; \psi_f^{\lambda\,*}(r)\, \psi_{\text{deut}}^\lambda(r) \Big|_{r=0} + \cdots$
- $f_L^{\text{from EFT}} \approx f_L^{\text{exact}}$
- Agreement made better by going to higher order terms in EFT expansion

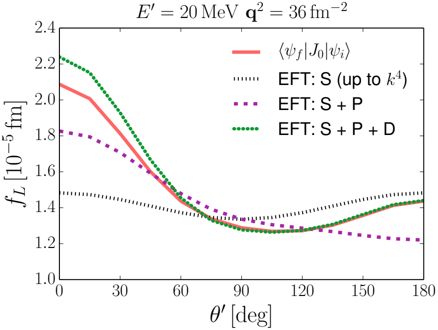

- $\langle \psi_f^\lambda | J_0^\lambda | \psi_{i\,^3S_1}^\lambda \rangle = \langle \psi_f^\lambda | ^3S_1 \rangle \langle ^3S_1 | J_0^\lambda | ^3S_1 \rangle \langle ^3S_1 | \psi_{i\,^3S_1}^\lambda \rangle + \sum_{J=0,1,2} \langle \psi_f^\lambda | ^3P_J \rangle \langle ^3P_J | J_0^\lambda | ^3S_1 \rangle \langle ^3S_1 | \psi_{i\,^3S_1}^\lambda \rangle + \sum_{J=1,2,3} \langle \psi_f^\lambda | ^3D_J \rangle \langle ^3D_J | J_0^\lambda | ^3S_1 \rangle \langle ^3S_1 | \psi_{i\,^3S_1}^\lambda \rangle$

Comparing power counting

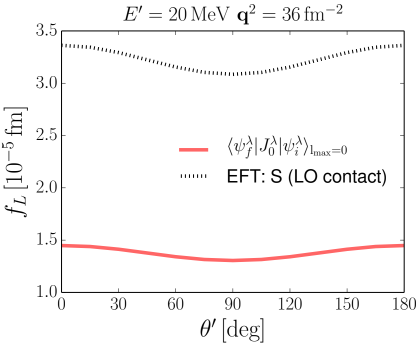

- $\langle\psi_f^\lambda|J_0^\lambda|\psi_i^\lambda\rangle_{l_{max}=0} \equiv \langle\psi_f^\lambda; {}^3S_1|J^\lambda_{0\ \text{exact}}|\psi_i^\lambda; {}^3S_1\rangle$
- $\langle{}^3S_1; k_1|J^\lambda_{0\ \text{EFT}}(q)|{}^3S_1; k_2\rangle = g_0^q + g_2^q\left(k_1^2 + k_2^2\right) + g_4^q\left(k_1^4 + k_2^4\right) + {g'_4}^q k_1^2 k_2^2$
- Large LO to NLO correction $\Rightarrow$ inefficient power counting

Comparing power counting

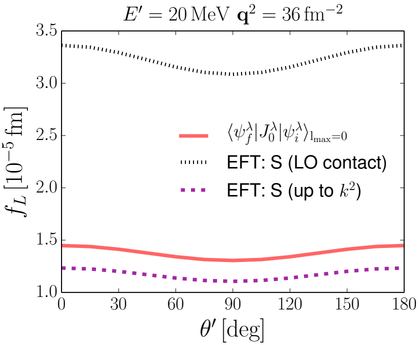

- $\langle\psi_f^\lambda|J_0^\lambda|\psi_i^\lambda\rangle_{\mathrm{l_{max}}=0} \equiv \langle\psi_f^\lambda;{}^3S_1|J^\lambda_{0\ \mathrm{exact}}|\psi_i^\lambda;{}^3S_1\rangle$
- $\langle{}^3S_1;k_1|J^\lambda_{0\ \mathrm{EFT}}(q)|{}^3S_1;k_2\rangle = g_0^q + g_2^q(k_1^2+k_2^2) + g_4^q(k_1^4+k_2^4) + g_4'^q k_1^2 k_2^2$
- Large LO to NLO correction ⇒ inefficient power counting

Comparing power counting

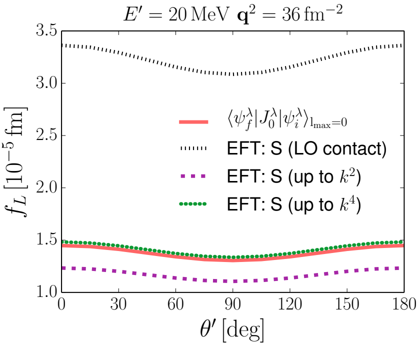

- $\langle\psi_f^\lambda|J_0^\lambda|\psi_i^\lambda\rangle_{l_{max}=0} \equiv \langle\psi_f^\lambda;{}^3S_1|J^\lambda_{0\,\text{exact}}|\psi_i^\lambda;{}^3S_1\rangle$
- $\langle{}^3S_1;k_1|J^\lambda_{0\,\text{EFT}}(q)|{}^3S_1;k_2\rangle = g_0^q + g_2^q(k_1^2+k_2^2) + g_4^q(k_1^4+k_2^4) + g_4'^q k_1^2 k_2^2$
- Large LO to NLO correction ⇒ inefficient power counting

Comparing power counting

- $\langle {}^3S_1; k_1 | J^{\lambda}_{0\,\mathrm{EFT}}(q) | {}^3S_1; k_2 \rangle =$
  $g_0^q + g_2^q(k_1^2 + k_2^2) + g_4^q(k_1^4 + k_2^4) + g_4'^q k_1^2 k_2^2$

$E' = 20$ MeV $\mathbf{q}^2 = 36\ \mathrm{fm}^{-2}$ $\langle \phi; {}^3S_1 \| J^{\lambda=1.5}_{0\,\mathrm{exact}} \| \psi_i^{\lambda}; {}^3S_1 \rangle = -0.005029$			
	LO	NLO	N^{2}LO
$\langle \phi; {}^3S_1 \| J^{\lambda}_{0\,\mathrm{EFT}} \| \psi_i^{\lambda}; {}^3S_1 \rangle$	-0.006479	-0.004826	-0.005004

Comparing power counting

- $\langle {}^3S_1; k_1 | J^{\lambda}_{0\,\mathrm{EFT}}(q) | {}^3S_1; k_2 \rangle =$
  $\left(g^q_0 + g^q_2\left(k_1^2 + k_2^2\right) + g^q_4\left(k_1^4 + k_2^4\right) + g'^q_4 k_1^2 k_2^2\right) e^{-ak^2/\lambda^2}$

$E' = 20$ MeV $\mathbf{q}^2 = 36$ fm^{-2} $\langle \phi; {}^3S_1 \| J^{\lambda=1.5}_{0\,\mathrm{exact}} \| \psi^{\lambda}_i; {}^3S_1 \rangle = -0.005029$			
	LO	NLO	N^{2}LO
$\langle \phi; {}^3S_1 \| J^{\lambda}_{0\,\mathrm{EFT}} \| \psi^{\lambda}_i; {}^3S_1 \rangle$	-0.006479	-0.004826	-0.005004
$\langle \phi; {}^3S_1 \| J^{\lambda}_{0\,\mathrm{SVD}} \| \psi^{\lambda}_i; {}^3S_1 \rangle$			

- Expansion in regulated contact terms obtained through singular value decomposition
- $J^{\lambda}_q(k', k) \xrightarrow{\mathrm{SVD}} \sum_i c^q_i j^i(k') j^i(k)$

Comparing power counting

- $\langle {}^3S_1; k_1 | J^{\lambda}_{0\,\mathrm{EFT}}(q) | {}^3S_1; k_2 \rangle =$
  $\left(g_0^q + g_2^q(k_1^2 + k_2^2) + g_4^q(k_1^4 + k_2^4) + g_4'^q k_1^2 k_2^2\right) e^{-ak^2/\lambda^2}$

$E' = 20$ MeV $\mathbf{q}^2 = 36$ fm^{-2} $\langle \phi; {}^3S_1 | J_{0\,\mathrm{exact}}^{\lambda=1.5} | \psi_i^{\lambda}; {}^3S_1 \rangle = -0.005029$			
	LO	NLO	$\mathrm{N^2LO}$
$\langle \phi; {}^3S_1 | J^{\lambda}_{0\,\mathrm{EFT}} | \psi_i^{\lambda}; {}^3S_1 \rangle$	-0.006479	-0.004826	-0.005004
$\langle \phi; {}^3S_1 | J^{\lambda}_{0\,\mathrm{SVD}} | \psi_i^{\lambda}; {}^3S_1 \rangle$	-0.005022		

- Expansion in regulated contact terms obtained through singular value decomposition
- $J_q^{\lambda}(k', k) \xrightarrow{\mathrm{SVD}} \sum_i c_i^q\, j^i(k') j^i(k)$

Comparing power counting

- $\langle {}^3S_1; k_1 | J^{\lambda}_{0\,\mathrm{EFT}}(q) | {}^3S_1; k_2 \rangle =$
$\left(g^q_0 + g^q_2\left(k_1^2 + k_2^2\right) + g^q_4\left(k_1^4 + k_2^4\right) + g'^q_4 k_1^2 k_2^2\right) e^{-ak^2/\lambda^2}$

$E' = 20$ MeV $\mathbf{q}^2 = 36$ fm^{-2} $\langle \phi; {}^3S_1 \| J^{\lambda=1.5}_{0\,\mathrm{exact}} \| \psi^{\lambda}_i; {}^3S_1 \rangle = -0.005029$			
	LO	NLO	N^{2}LO
$\langle \phi; {}^3S_1 \| J^{\lambda}_{0\,\mathrm{EFT}} \| \psi^{\lambda}_i; {}^3S_1 \rangle$	-0.006479	-0.004826	-0.005004
$\langle \phi; {}^3S_1 \| J^{\lambda}_{0\,\mathrm{SVD}} \| \psi^{\lambda}_i; {}^3S_1 \rangle$	-0.005022	-0.005055	

- Expansion in regulated contact terms obtained through singular value decomposition
- $J^{\lambda}_q(k', k) \xrightarrow{\mathrm{SVD}} \sum_i c^q_i j^i(k') j^i(k)$

Comparing power counting

- $\langle {}^3S_1; k_1 | J^{\lambda}_{0\,\mathrm{EFT}}(q) | {}^3S_1; k_2 \rangle =$
  $\left(g^q_0 + g^q_2(k_1^2 + k_2^2) + g^q_4(k_1^4 + k_2^4) + g'^q_4 k_1^2 k_2^2\right) e^{-ak^2/\lambda^2}$

$E' = 20$ MeV $\mathbf{q}^2 = 36$ fm^{-2} $\langle \phi; {}^3S_1 \vert J^{\lambda=1.5}_{0\,\mathrm{exact}} \vert \psi^{\lambda}_i; {}^3S_1 \rangle = -0.005029$			
	LO	NLO	N^{2}LO
$\langle \phi; {}^3S_1 \vert J^{\lambda}_{0\,\mathrm{EFT}} \vert \psi^{\lambda}_i; {}^3S_1 \rangle$	-0.006479	-0.004826	-0.005004
$\langle \phi; {}^3S_1 \vert J^{\lambda}_{0\,\mathrm{SVD}} \vert \psi^{\lambda}_i; {}^3S_1 \rangle$	-0.005022	-0.005055	-0.005028

- Expansion in regulated contact terms obtained through singular value decomposition
- $J^{\lambda}_q(k', k) \xrightarrow{\mathrm{SVD}} \sum_i c^q_i\, j^i(k') j^i(k)$

q-factorization of f_L

- $f_L \equiv f_L(p', \theta; q)$
  p' and θ: outgoing nucleon
  q: momentum transfer
- For $p' \ll q$, f_L scales with q
  $f_L(p', \theta; q) \to g(p', \theta)B(q)$
- Note that f_L is a strong function of q

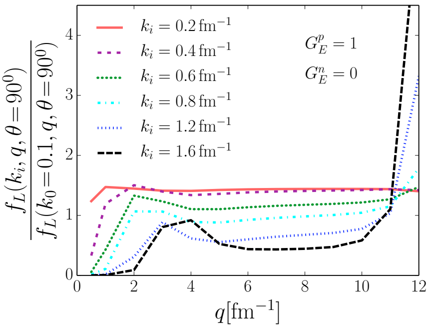

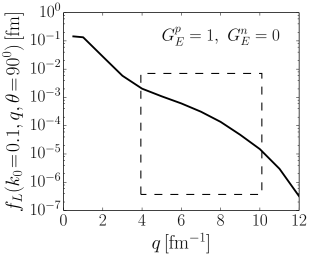

q-factorization of f_L

- $f_L \equiv f_L(p', \theta; q)$
  p' and θ: outgoing nucleon
  q: momentum transfer
- For $p' \ll q$, f_L scales with q
  $f_L(p', \theta; q) \rightarrow g(p', \theta) B(q)$
- Note that f_L is a strong function of q
- Follows from the LO term in SVD expansion:
  $\langle \psi_f^\lambda | J_0^\lambda(q) | \psi_{\rm deut}^\lambda \rangle \approx c_0^q \; \psi_f^{\lambda *}(p'; r)\, \psi_{\rm deut}^\lambda(r) \Big|_{r=0}$

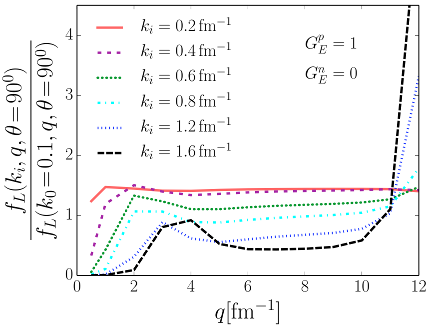

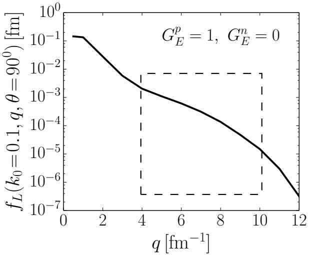

Scale dependent D-state contribution

- Sensitivity of observables to the deuteron D-state probability
- Surrey group: sensitivity to high-*np* momenta and D-state component in (d, p) reactions [e.g., PRL **117** (2016)]

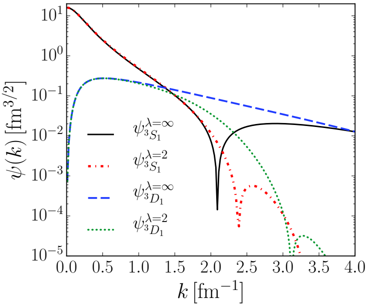

Scale dependent D-state contribution

- Sensitivity of observables to the deuteron D-state probability
- Surrey group: sensitivity to high-*np* momenta and D-state component in (d, p) reactions [e.g., PRL **117** (2016)]

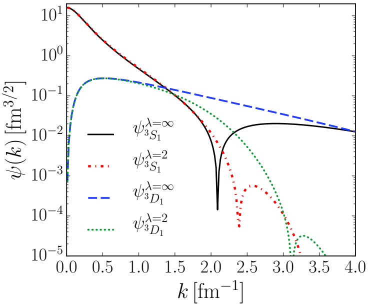

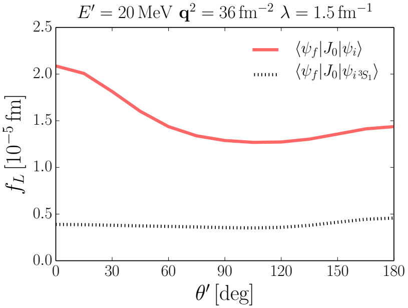

Scale dependent D-state contribution

- Sensitivity of observables to the deuteron D-state probability
- Surrey group: sensitivity to high-*np* momenta and D-state component in (d,p) reactions [e.g., PRL **117** (2016)]

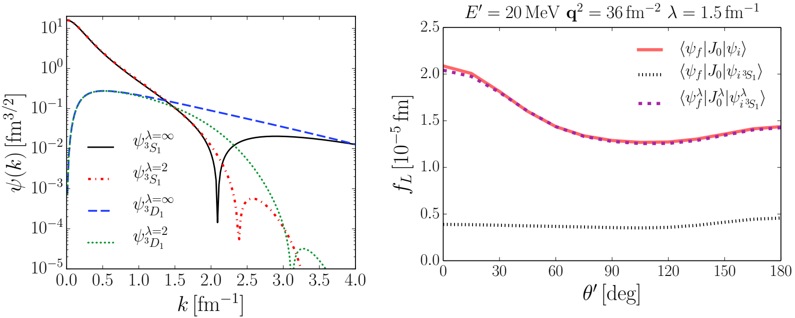

- Unevolved contribution to f_L mostly *D*-state but all *S*-state for evolved

Scale dependent D-state contribution

- Sensitivity of observables to the deuteron D-state probability
- Surrey group: sensitivity to high-*np* momenta and D-state component in (d,p) reactions [e.g., PRL **117** (2016)]

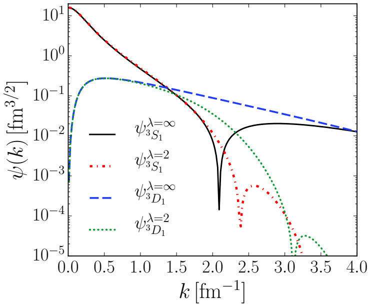

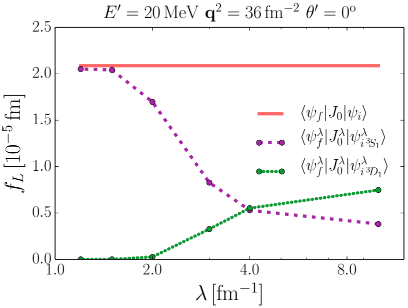

- Unevolved contribution to f_L mostly *D*-state but all *S*-state for evolved
- λ evolution shows switch from *D*-channel to *S*-channel

Summary

Case study shows:

- Scale dependence abounds... in a systematic way which can be accounted for
- Underlying physics is scale dependent not just kinematics dependent
  - Sensitivity to specific component of nuclear wave function can be highly scale dependent
  - Local decoupling + form of evolved current $\rightarrow$ reduced FSI at low resolutions
- Conventional wisdom: low-resolution potentials ill-suited for (high-q) reactions calculations ✗
  $\rightarrow$ RG changes to $\widehat{O}_q$ tractable
- Explanation of factorization straightforward in low-momentum picture

Summary

Case study shows:

- Scale dependence abounds... in a systematic way which can be accounted for
- Underlying physics is scale dependent not just kinematics dependent
  - Sensitivity to specific component of nuclear wave function can be highly scale dependent
  - Local decoupling + form of evolved current $\rightarrow$ reduced FSI at low resolutions
- Conventional wisdom: low-resolution potentials ill-suited for (high-q) reactions calculations ✗
  $\rightarrow$ RG changes to $\widehat{O}_q$ tractable
- Explanation of factorization straightforward in low-momentum picture

To do:

- Make the EFT picture for J_0^λ more quantitative, explore SVD
- Include initial two-body currents, extend to $A > 2$, connect to other nuclear processes
- Basis for consistent construction of operators

Relevance to $0\nu\beta\beta$

- Evolution of leading $0\nu\beta\beta$ operator
  $\rightarrow$ Extract EFTish picture
- Factorization arguments
  $\rightarrow$ understand the SRC factor
  $\rightarrow$ correlation among various observables
- Scale dependence of g_A

Back up

Cartoon picture

kinematics	before	after
quasielastic	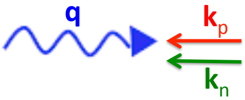	
high $\mathbf{q}^2$, low E' at $\lambda = \infty$	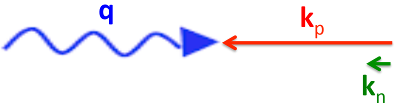	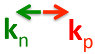
high $\mathbf{q}^2$, low E' at small λ	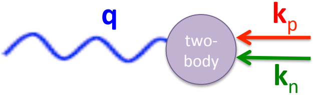	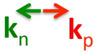

EMC Phenomenology

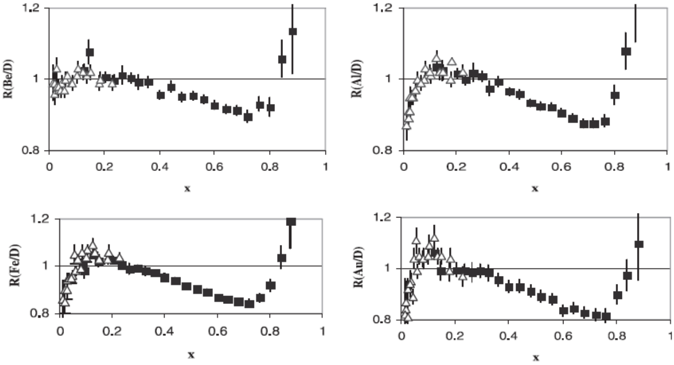

Notron, Rep. Prog. Phys. (2003) (data from SLAC)

- EMC ⇒ nuclear modification of nucleonic properties. The EMC ratio is independent of Q^2.
- The shape is universal: independent of A. Depletion at small x, greater than 1 for $0.1 < x < 0.3$, linear fall for $0.3 < x < 0.7$ and steep rise for $x > 0.7$.
- The magnitude of distortion is A dependent. It goes roughly as ρ_A.

QCD non-perturbative at low energies

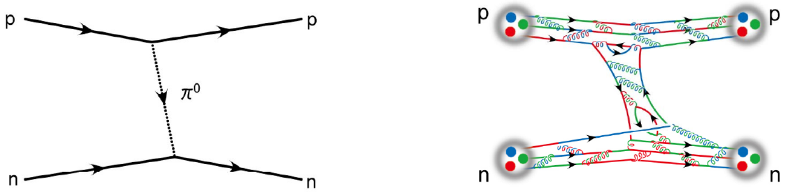

- QCD is underlying theory

QCD non-perturbative at low energies

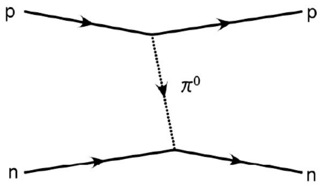

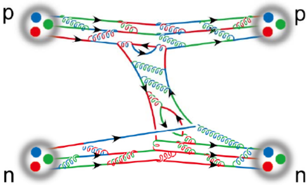

- QCD is underlying theory
- Nuclear energies: $\sim$ few MeVs
- QCD non-perturbative at low energies

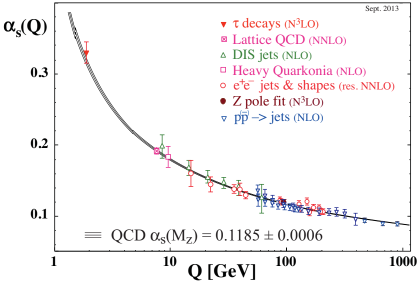

Shell model

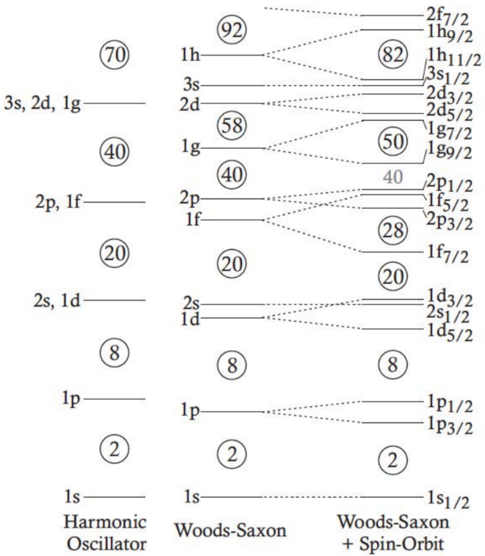
70
40
20
8
2
3s, 2d, 1g
2p, 1f
2s, 1d
1p
1s
Harmonic Oscillator
92
58
40
20
8
2
1h
3s
2d
1g
2p
1f
2s
1d
1p
1s
Woods-Saxon
82
50
40
28
20
8
2
2f7/2
1h9/2
1h11/2
3s1/2
2d3/2
2d5/2
1g7/2
1g9/2
2p1/2
1f5/2
2p3/2
1f7/2
1d3/2
2s1/2
1d5/2
1p1/2
1p3/2
1s1/2
Woods-Saxon + Spin-Orbit

Choose appropriate degrees of freedom

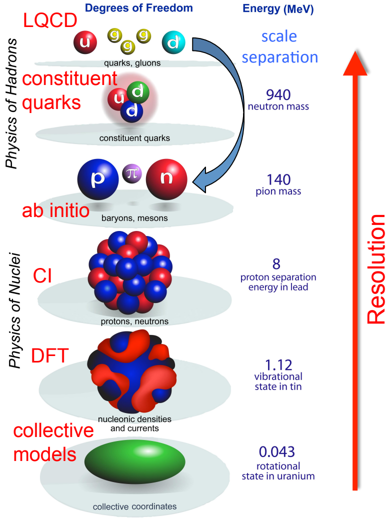

"You may use any degrees of freedom you like to describe a physical system, but if you use the wrong ones, you'll be sorry!" - Weinberg

Chiral EFT diagrams

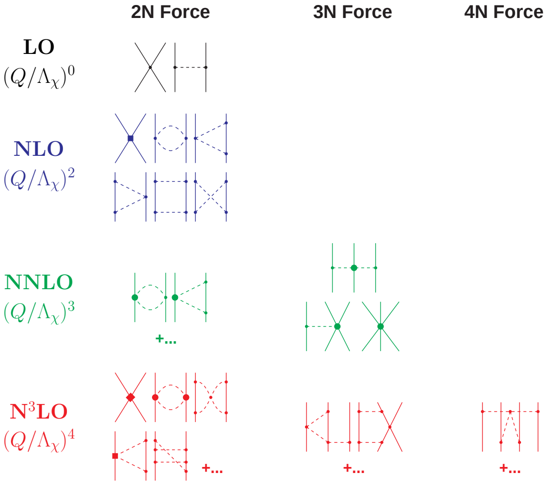

SRG back up

- SRG flow equation: $\frac{dH_s}{ds} = [[T_{\rm rel}\,,\,H_s]\,,\,H_s]$
- s: flow parameter. $T_{\rm rel}$: relative kinetic energy
- $E_n = \langle\Psi_n|H|\Psi_n\rangle = (\langle\Psi_n|U_s^\dagger)U_sHU_s^\dagger(U_s|\Psi_n\rangle) = \langle\Psi_n^s|H_s|\Psi_n^s\rangle$
- There is no unique potential!
- $\lambda^2 = 1/\sqrt{s}$
- $\frac{dV_\lambda}{d\lambda}(k,k') \propto -(\epsilon_k - \epsilon_{k'})^2 V_\lambda(k,k') + \sum_q (\epsilon_k + \epsilon_{k'} - 2\epsilon_q) V_\lambda(k,q) V_\lambda(q,k')$
- $O_s = U_s\, O\, U_s^\dagger$
- $\frac{d\,O_s}{d\,s} = [[G_s\,,\,H_s]\,,O_s]$
- $\frac{d\,U_s}{d\,s} = [G_s\,,\,H_s]\,U_s$
- $U_s = \sum_i |\psi_i(s)\rangle\langle\psi_i(0)|$

Tjon line

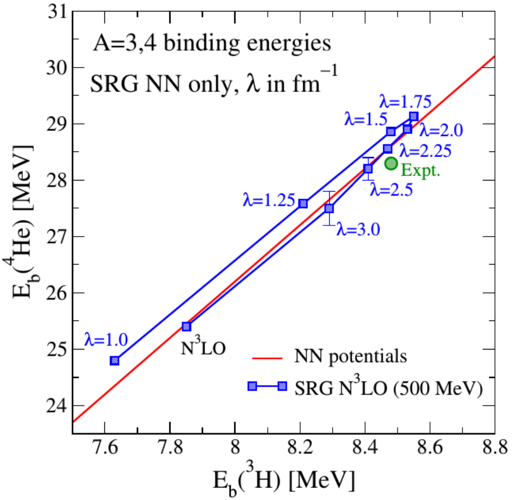

A=3,4 binding energies
SRG NN only, λ in fm⁻¹
λ=1.0
λ=1.25
λ=1.5
λ=1.75
λ=2.0
λ=2.25
λ=2.5
λ=3.0
Expt.
N³LO
NN potentials
SRG N³LO (500 MeV)
E_b(⁴He) [MeV]
E_b(³H) [MeV]
24
25
26
27
28
29
30
31
7.6
7.8
8
8.2
8.4
8.6
8.8

Numerical implementation

- $\langle\phi|t_\lambda^\dagger\, G_0^\dagger\, J_0^\lambda|\psi_i^\lambda\rangle = \langle\phi|t_\lambda^\dagger\, G_0^\dagger\, \widetilde{U}\, J_0\, \widetilde{U}^\dagger|\psi_i^\lambda\rangle + \cdots$
- $U = I + \widetilde{U}$. Smooth $\widetilde{U}$ amenable to interpolation.
- Insert complete set of partial wave basis of the form
  $$1 = \frac{2}{\pi} \sum_{\substack{L,S \\ J,m_J}} \sum_{T=0,1} \int dp\, p^2\, |p\, J\, m_J\, L\, S\, T\rangle\, \langle p\, J\, m_J\, L\, S\, T|\ .$$
- Large number of nested sums and integrals. Caching techniques used to avoid recalculation of t-matrix.
- Parallelization implemented using TBB library. Run on a node with 48 cores.

Numerical implementation: representative term

$$
\begin{aligned}
\langle\phi|t_\lambda^\dagger\, G_0^\dagger\, \widetilde{U}\, J_0\, \widetilde{U}^\dagger|\psi_i^\lambda\rangle &= \frac{8}{\pi^2}\sqrt{\frac{2}{\pi}}\,\frac{M}{\hbar c}\int\frac{\mathrm{d}k_2\,k_2^2}{(p'+k_2)(p'-k_2-i\epsilon)}\sum_{T_1=0,1}\left(G_E^p+(-1)^{T_1}\,G_E^n\right)\\
&\times\sum_{L_1=0}^{L_{\max}}\left(1+(-1)^{T_1}(-1)^{L_1}\right)\times Y_{L_1,m_{J_d}-m_{s_f}}(\theta',\varphi')\sum_{J_1=|L_1-1|}^{L+1}\langle L_1\,m_{J_d}-m_{s_f}\,S=1\,m_{s_f}|J_1\,m_{J_d}\rangle\\
&\times\sum_{L_2=0}^{L_{\max}}t_\lambda^*(k_2,p',L_2,L_1,J_1,S=1,T_1)\sum_{L_3=0}^{L_{\max}}\sum_{\widetilde{m}_s=-1}^{1}\langle J_1\,m_{J_d}\,L_3\,m_{J_d}-\widetilde{m}_s|S=1\,\widetilde{m}_s\rangle\\
&\times\sum_{L_4=0}^{L_{\max}}\langle L_4\,m_{J_d}-\widetilde{m}_s\,S=1\,\widetilde{m}_s|J=1\,m_{J_d}\rangle\int\mathrm{d}k_4\,k_4^2\,\widetilde{U}(k_2,k_4,L_2,L_3,J_1,S=1,T_1)\\
&\times\int\mathrm{d}\cos\theta\,P_{L_3}^{m_{J_d}-\widetilde{m}_s}(\cos\theta)\,P_{L_4}^{m_{J_d}-\widetilde{m}_s}\left(\cos\alpha'(k_4,\theta)\right)\\
&\times\int\mathrm{d}k_6\,k_6^2\sum_{L_d=0,2}\widetilde{U}\left(k_6,\sqrt{{k_4}^2-k_4q\cos\theta+q^2/4},L_d,L_4,J=1,S=1,T=0\right)\psi_{L_d}^\lambda(k_6)\,.
\end{aligned}
$$